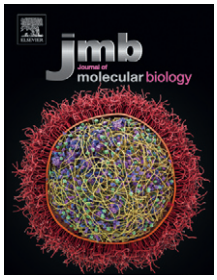

Microsecond Rearrangements of Hydrophobic Clusters in an Initially Collapsed Globule Prime Structure Formation during the Folding of a Small Protein

Rama Reddy Goluguri and Jayant B. Udgaonkar

National Centre for Biological Sciences, *Tata Institute of Fundamental Research, Bengaluru 560065, India*

Correspondence to Jayant B. Udgaonkar: *jayant@ncbs.res.in*
http://dx.doi.org/10.1016/j.jmb.2016.06.015
Edited by Sheena Radford

Abstract

Determining how polypeptide chain collapse initiates structure formation during protein folding is a long standing goal. It has been challenging to characterize experimentally the dynamics of the polypeptide chain, which lead to the formation of a compact kinetic molten globule (MG) in about a millisecond. In this study, the sub-millisecond events that occur early during the folding of monellin from the guanidine hydrochloride-unfolded state have been characterized using multiple fluorescence and fluorescence resonance energy transfer probes. The kinetic MG is shown to form in a noncooperative manner from the unfolded (U) state as a result of at least three different processes happening during the first millisecond of folding. Initial chain compaction completes within the first 37 μs, and further compaction occurs only after structure formation commences at a few milliseconds of folding. The transient nonnative and native-like hydrophobic clusters with side chains of certain residues buried form during the initial chain collapse and the nonnative clusters quickly disassemble. Subsequently, partial chain desolvation occurs, leading to the formation of a kinetic MG. The initial chain compaction and subsequent chain rearrangement appear to be barrierless processes. The two structural rearrangements within the collapsed globule appear to prime the protein for the actual folding transition.

Introduction

The defining event on the folding pathways of many proteins is the formation of the molten globule (MG) conformation, which is usually complete by a few milliseconds of folding [1–3]. At this critical juncture during folding, immediately preceding the major structure formation reactions, the polypeptide chain has partially compacted [2,4], has gained some specific structure, including secondary structure [5,6], is likely to have already adopted a native-like topology [7,8], but is still liquid-like in its conformational dynamics. The malleability of the structures of kinetic MGs results in them being tunable by a change in folding conditions [4,9–11]. Kinetic MGs may contain nonnative structure [12,13], but how nonnative structure forms and modulates folding is not clearly known. It is from the kinetic MG that most of the protein structure will slowly evolve, ultimately leading to the tightly packed, solid-like native state (N state) that confers function to the protein. Understanding the dynamics of the protein chain, which lead to the formation of the kinetic MG, is crucial for understanding how structure formation is seeded during the initiation of protein folding.

Continuous-flow, microsecond mixing studies of the folding of several proteins [14–21] have shown that the initial contraction of the polypeptide chain is usually complete within the mixing dead time, which can be as short as 10 μs. Other studies, in which folding was initiated with even faster time resolution, suggested that initial chain contraction might actually occur on the 100-ns timescale [22,23]. The initial contraction of the fully unfolded (U) form in high denaturant to the U form in refolding conditions (U_C) has been likened to the coil-to-globule collapse of a homopolymer chain that occurs upon transfer from good to bad solvent [24–26]. Is protein chain contraction indeed a non-specific [4,27–29], second

order [20,29–33] process governed by excluded volume effects, chain entropy, and a few stabilizing but nonnative enthalpic interactions? [3,34] Or does the evolutionarily designed heteropolymer chain contract by a barrier-limited process, in which some but not all protein molecules collapse, with contraction being driven by at least some native interactions, thereby leading to at least some native structure? [16–18,35–37] Does chain collapse lead to concomitant formation of specific secondary structure, as predicted by some theoretical studies [38,39], or does chain collapse precede secondary structure formation, as seen in some experimental studies? [4,29,33,40–43] It is not known whether it is the sequence of the protein chain that determines the extent to which initial chain contraction occurs and why different segments of the chain compact to different extents [31,44,45]. Finally, it is not known whether the contraction is driven by only hydrophobic interactions [4,46,47], whether hydrogen-bonding interactions also play a significant role [48,49], and to what extent these interactions are nonnative [13].

After the initial chain compaction to U_C, which is completed in the 100-ns to 10-μs time domain, the polypeptide chain is likely to undergo rearrangements that lead to the formation of the kinetic MG in the 10-μs to 10-ms time domain. Diffusive motions of the polypeptide chain in compact denatured protein conformations are known to occur in the 10-to-100-μs time domain [50–52] and are expected to be slowed down by internal friction [53], hydrodynamic effects, and by the transient formation and breakage of many enthalpic interactions [54]. Little is known about whether further chain contraction occurs during this diffusive meandering of the protein chain as U_C transforms into the kinetic MG and to what extent chain desolvation occurs. Is the diffusive process limited in rate by significant free energy barriers [53], or is it a gradual barrierless process as some studies indicate? [20] In particular, the role played by long-range interactions, whether native or nonnative, is not understood. How such interactions along with steric effects come into play in inducing and stabilizing secondary structure during the formation of the kinetic MG [38] is still to be understood. To better understand how a kinetic MG becomes primed to fold during the process of its formation, it is necessary to dissect the sub-millisecond folding process into individual steps using multiple structural probes.

The small plant protein monellin (MNEI) is known to fold via a kinetic molten MG that offers itself as an attractive system for understanding how kinetic MGs form [16,45]. The kinetic MG of MNEI is devoid of the helical structure present in N state, and its different sequence segments unfold noncooperatively and have different stabilities [45]. It appears to possess some specific structure, as judged by its shape monitored by small angle X-ray scattering (SAXS) [16] and by the observation that some, but not all, intramolecular distances within it have contracted more than expected by the denaturant dilution [45]. Understanding the chain rearrangements that lead to the formation of the kinetic MG of MNEI will lead to a better understanding of how helical structure begins to form from a protein denatured state [45] of the heterogeneity inherent in the kinetic MG ensemble [8,11] and how such heterogeneity might lead to subsequent structure formation occurring along multiple folding routes [55,56].

In the current study, the sub-millisecond folding reactions of MNEI were studied using a custom-built, continuous-flow setup with a mixing dead time of 37 μs. The folding reaction of MNEI was initiated from the guanidine hydrochloride (GdnHCl)-unfolded state and was monitored by intrinsic tryptophan fluorescence, multisite fluorescence resonance energy transfer (FRET), fluorescence of an 5-((((2-iodoacetyl) amino)-ethyl)amino)-naphthalene-1-sulfonic acid (IAEDANS) adduct on the protein, and by 1-anilino napthalene8-sulfonate (ANS) fluorescence. For multisite FRET measurements, the single tryptophan at residue position 4 was used as the donor fluorophore, and a thionitrobenzoate (TNB) moiety attached to cysteine residues located at different parts of the protein in different single-cysteine-containing mutant variants of MNEI was used as an acceptor (Fig. 1). The sub-millisecond folding reaction occurs in at least three distinct kinetic phases. The initial collapse transition is over within the mixing dead time, giving an upper limit of ~10 μs to the time constant for the coil-to-globule transition in MNEI. Surprisingly, the collapsed globule has already formed hydrophobic

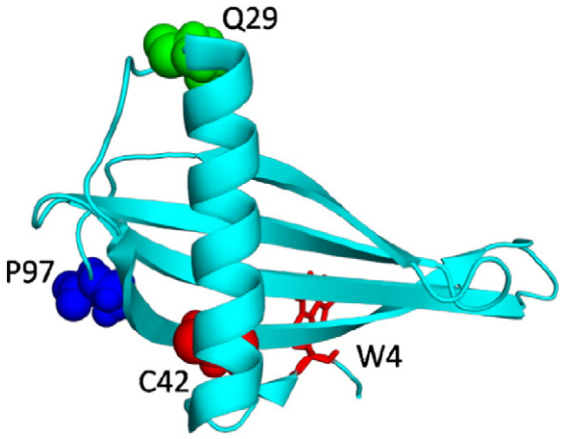

Fig. 1. Structure of single-chain monellin. The positions of the residues, which were mutated to cysteine (spheres) in the different single-cysteine-containing mutant forms of MNEI used for the multisite FRET measurements, are shown. The structure was drawn from the PDB entry 1FA3 using PYMOL. The single tryptophan residue (W4) used as the donor fluorophore is also shown (sticks).

patches that can bind the hydrophobic dye, ANS. The sole tryptophan in the protein has undergone nonnative burial in U_C. The collapsed globule undergoes two consecutive structural transitions, one accompanied by a hyperfast decrease in tryptophan fluorescence and the other by an ultrafast decrease in the fluorescence of ANS, which leads to the formation of the kinetic MG.

Results

W4 shows hyperfluorescence within the 37-μs dead time

When refolding was initiated using the microsecond mixer, the single tryptophan residue 4 (W4) in MNEI showed an increase in fluorescence within the 37 μs dead time of the microsecond mixer. Since the entire signal change in tryptophan fluorescence, which is seen upon the folding of U to N, could be captured by stopped-flow mixing, it was surprising to observe this transient burst-phase increase in fluorescence in the microsecond time domain (Fig. 2). The fluorescence emission spectrum also appeared to show a blue shift relative to the fluorescence spectrum of the U state, which shows maximum fluorescence at 355 nm [55]. The amplitude of the burst phase of hyperfluorescence was more at 340 nm than at 360 nm (Fig. 2a and b). The amplitude of this burst phase decreased with an increase in GdnHCl concentration (Fig. 2c). It should be noted that the fluorescence of the U state of MNEI in 4 M GdnHCl is 0.95 times that of the fluorescence of *N*-acetyl-L-tryptophanamide (NATA) in 4 M GdnHCl at 340 nm and is 0.85 times that of the fluorescence of NATA in 4 M GdnHCl at 360 nm.

The tryptophan fluorescence then decreased in a hyperfast kinetic phase with a time constant of 50 ± 10 μs in 0.86 M GdnHCl. The rate constant for this hyperfast phase decreased with an increase in GdnHCl concentration (Fig. 2d). Further changes in tryptophan fluorescence, in three kinetic phases of folding, were observed in the millisecond-to-second time domain upon stopped-flow mixing (Fig. 2d), and the three rate constants of the three kinetic phases were found to be similar in values to the values published earlier [45,55].

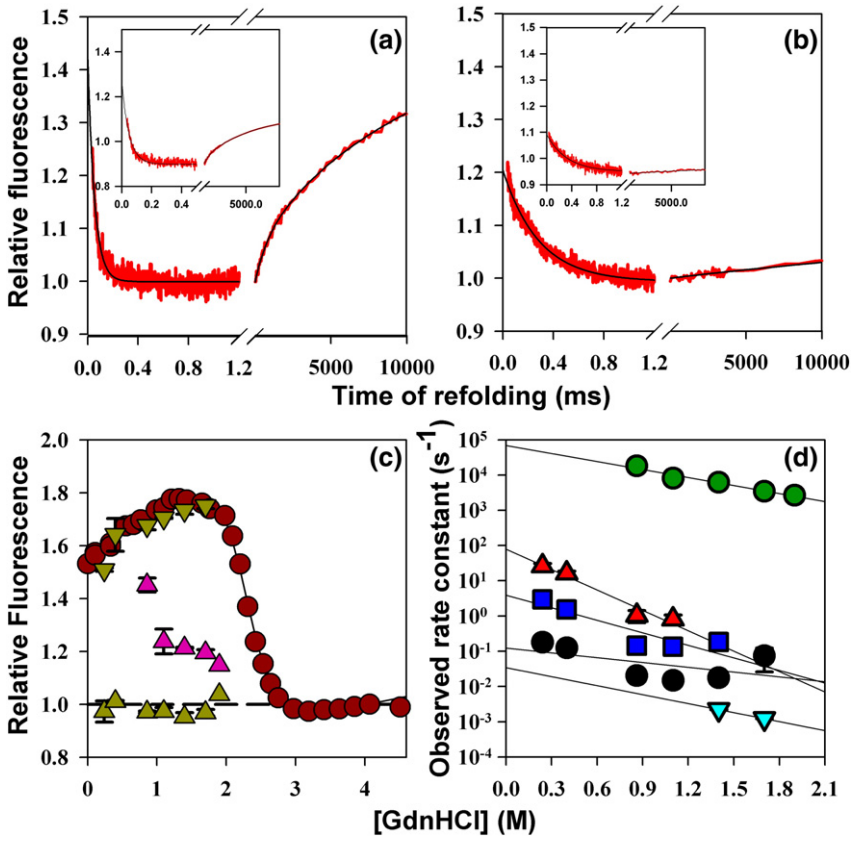

Fig. 2. Refolding of MNEI (Cys42) monitored by tryptophan fluorescence. (a) Representative kinetic trace of folding in 0.86 M GdnHCl obtained by monitoring the tryptophan fluorescence at 340 nm after continuous-flow mixing. The kinetic trace obtained using stopped-flow mixing under identical conditions is shown after the *x*-axis break. (b) Representative kinetic trace at 1.7 M GdnHCl. The insets in panels (a and b) show the kinetic traces monitored by fluorescence emission at 360 nm. The signals were normalized to the value of 1 for the fluorescence signal of the protein in 4 M GdnHCl. (c) Comparison of the equilibrium and kinetic amplitudes of the fluorescence change at 340 nm.●, the equilibrium transition; ▲, the $t = 0$ points of the stopped-flow kinetic traces; ▲, the $t = 0$ points of sub-millisecond, continuous-flow kinetic traces; ▼, $t = \infty$ signals of the stopped-flow traces. The discontinuous black line represents the signal of the unfolded protein in 4 M GdnHCl. (d) Comparison of the rate constants of different refolding phases observed by both stopped-flow and continuous-flow mixing, by measurement of the tryptophan fluorescence at 340 nm. ●, hyperfast phase; ▲, very fast phase; ■, fast phase; ● , slow phase; ▼, very slow phase.

In order to study how the different segments of the polypeptide chain undergo compaction during the sub-millisecond time domain by FRET, three single-tryptophan- and single-cysteine-containing variants of MNEI were prepared (Fig. 1). In all the three MNEI variants, W4 was used as the donor (D) fluorophore, and a TNB attached to the cysteine at a specific location in each mutant variant was used as the acceptor (A). For all three TNB-labeled proteins, Cys29-TNB, Cys42-TNB, and Cys97-TNB, the sub-millisecond kinetic traces of folding obtained from continuous-flow mixing merged into the kinetic traces obtained from stopped-flow mixing (Fig. S3a–c). The kinetic traces of folding of all three TNB-labeled proteins extrapolated at $t = 0$ to the fluorescence value of U protein in 4 M GdnHCl (Fig. S3a–c). The decrease in tryptophan fluorescence for each TNB-labeled protein occurred in the hyperfast phase: the rate constants were found to be similar to the rate constants obtained for the corresponding unlabeled protein (Fig. 3), whose tryptophan hyperfluorescence decreased in this phase (Fig. 2).

In order to understand the nature of barriers that slow down the sub-millisecond dynamics of the protein, the microsecond mixing refolding experiments were carried out at different temperatures. The activation energies for the sub-millisecond dynamics of the three different segments of the protein were determined for Cys29-TNB, Cys42-TNB, and Cys97-TNB from Arrhenius plots and had values of 5.2 kcal/mol, 6.7 kcal/mol, and 5.2 kcal/mol, respectively (Fig. S3d).

MNEI undergoes compaction within 37 μs of the initiation of folding

The change in FRET efficiency during sub-millisecond folding was calculated from the kinetic

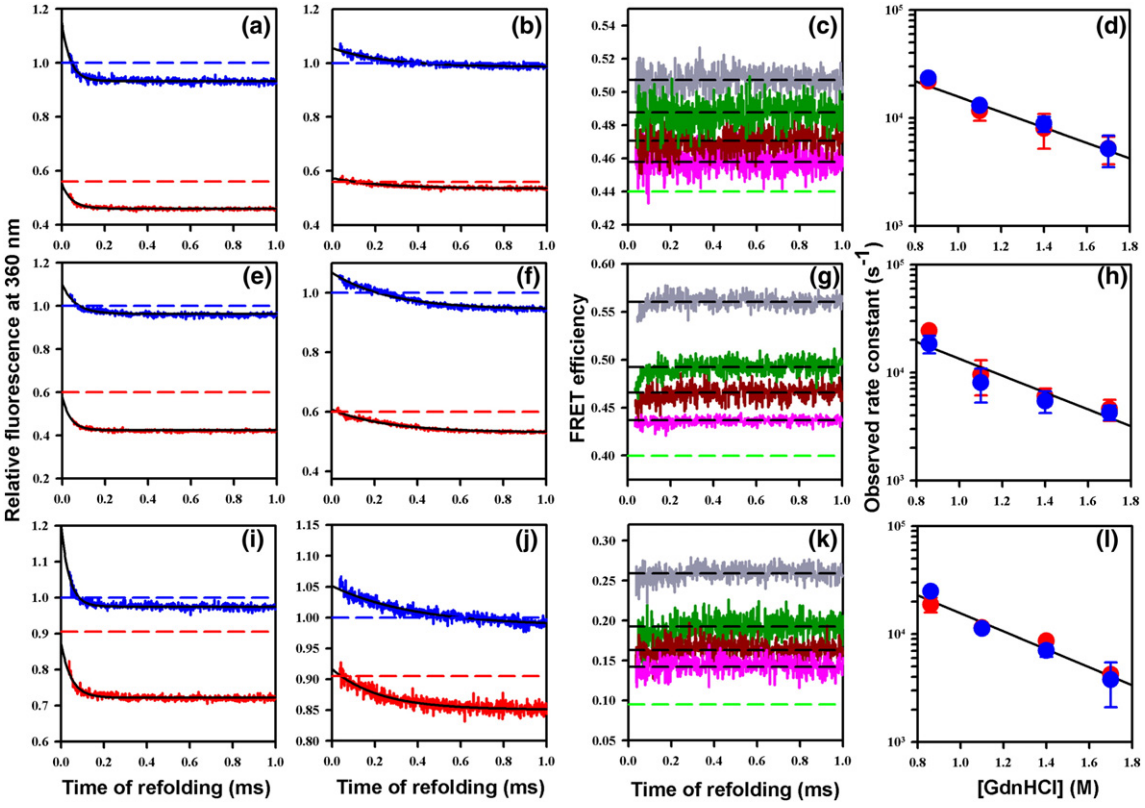

Fig. 3. Sub-millisecond refolding kinetic traces of different TNB-labeled and unlabeled variants of MNEI. The kinetic traces were obtained by monitoring tryptophan fluorescence at 360 nm upon excitation at 295 nm. The data for the W4-C29 (a–d), W4-C42 (e–h), and W4-C97 (i–l) distances of MNEI were measured using Cys29 and Cys29-TNB, Cys42 and Cys42-TNB, and Cys97 and Cys97-TNB, respectively**.** Panels (a, e, and i) represent kinetic refolding traces in 0.86 M GdnHCl, and panels (b, f, and j) represent kinetic refolding traces in 1.7 M GdnHCl for both unlabeled (blue) and labeled (red) proteins. The dashed blue and red lines in panels (a, b, e, f, i, and j) represent the signals for the unlabeled and labeled proteins, respectively, in 4 M GdnHCl. FRET efficiency monitored the kinetic traces that are shown in panels (c, g, and k) for folding in 0.86 (gray), 1.1 (green), 1.4 (dark red), and 1.7 (pink) M GdnHCl. The FRET efficiency in the U state in 4 M GdnHCl is shown as a dashed green line. The mean FRET efficiencies are shown as dashed black lines through the data, as shown in panels (c, g, and k). Panels (d, h, and l) compare the rates of hyperfast fluorescence change for the labeled (red) and unlabeled (blue) proteins.

traces of labeled (F_{DA}) and unlabeled (F_D) proteins for the three segments of the protein (W4-C29, W4-C42, W4-C97). For each of these segments, the FRET efficiency increased within the 37-μs burst phase (Fig. 3) and then remained constant from 37 μs to 1.4 ms (Fig. 3), changing further only due to the folding transition that occurred at longer times.

Strictly speaking, the FRET efficiency needs to be calculated from the ratio of fluorescence quantum yields of the FRET donor in the absence and presence of the FRET acceptor. In practice, however, FRET efficiency changes during folding are invariably determined using the fluorescence intensities, not the quantum yields, at one particular wavelength [32,33,35,40]. In order to make sure that the ratio of fluorescence intensities of the donor in the absence and presence of acceptor, at a particular wavelength, correctly represents the ratio of quantum yields, it is important to demonstrate that the same value for the FRET efficiency was obtained for the initially collapsed form (U_C), when intensities were measured at a second wavelength [31]. Figure S4 shows that this is indeed the case: the FRET efficiency in U_C for the W4-C42 segment of the protein was the same whether the fluorescence intensities were measured at 340 nm or at 360 nm. Since all the three distances probed showed increases in FRET efficiency during the 37-μs burst phase, it was concluded that the volume of the polypeptide chain had decreased due to initial polypeptide chain collapse.

The increase in FRET efficiency accompanying the collapse of U to U_C was found to be different for the different FRET pairs (Table S1), indicating that different distances had contracted to different extents. Furthermore, the increase in FRET efficiency for each segment was found to be independent of the final FRET efficiency in the N state, suggesting that U_C was a randomly collapsed globule. In order to estimate the extents of contraction for different segments of the protein during the 37-μs burst phase, the FRET efficiencies determined for U and U_C were converted into distances using Eq. (1), with the previously determined value for R_0 of 22.5 Å [57]. In using Eq. (1), it was assumed that the distribution of intramolecular distances in both U and U_C was a Gaussian distribution (see Supplementary Data).

For the U state, which is an ensemble of states that interconvert on the time scale of few μs [58], the assumption of a Gaussian distribution for each of the three chain segments encompassing the FRET pair allowed the value of the radius of gyration, R_g, to be calculated for the whole protein (see Supplementary Data). The average of the three estimates for R_g, 22.5 ± 2.6 Å, is similar in value to the value of R_g determined by SAXS in a previous study [16], pointing to the validity of the Gaussian chain model for the U state. More importantly, for every protein segment defined by W4 at one end and a TNB moiety attached to a Cys residue at the other end, the dependence of the segment-wise R_g values (albeit only three in number) on the number of residues, N, separating the Trp and Cys residues in the segment, yielded a value for the scaling exponent, v (R_g α N^v), of 0.59 (Fig. S5a), which is close to the value (0.6) expected for a random coil [24]. In this context, it is important to note that for other proteins, it appears that the Gaussian chain model may not be appropriate for describing the dimensions of the U state [59,60].

For the U_C state, there were two potential problems in using the FRET data to determine intramolecular distances and R_g. Firstly, the value of R_0, which is given by Eq. (2), may not be the same for U_C and U. This is because W4 is partially buried, as indicated by its hyperfluorescence, in U_C (see above) but not in U state. Hence, the value of Q_D [Eq. (2)] for U_C is higher than that for U, but it is only 1.2- to 1.3-fold higher (Fig. 2), and since R_0 α $Q_D^{1/6}$ [Eq. (2)], there will be a negligible effect on the value of R_0. The partial burial of W4 in U_C may have also affected its dynamics and hence altered the value of κ^2 [Eq. (2)], which was assumed to have a value of 2/3 as in the U state, in which W4 and the TNB moiety would be randomly oriented with respect to each other. Nevertheless, since U_C appears to be a randomly collapsed globule (see above), it is likely that the value of 2/3 for of κ^2 may still be applicable. In any case, R_0 α $(\kappa^2)^{1/6}$; consequently, the effect of a small change in κ^2 on R_0 should be small. Secondly, there may be specific interactions and structures present in U_C, as suggested by the observation that the W4-C42 and W4-C97 segments have contracted more than expected from a mere solvent change [45]. Although a fully unfolded protein chain may be describable as a Gaussian chain, even when it might possess significant amounts of structure [61], it is unlikely that a collapsed chain would be similarly describable if structure were to be present. These structures might affect the dynamics of the chain. Not surprisingly, the three estimates for the value of R_g of the whole protein in the U_C state, obtained using the Gaussian distribution assumption for U_C, were found to vary over a large range, from 13.2 to 19.6 Å (Table S1), and the scaling exponent, v, obtained from the dependence of the segment-wise R_g values (albeit only three in number) on length of segment (N) had a value of 0.24 (Fig. S5b), and not 0.33, as expected for a collapsed globule [24]. It should be noted that a scaling exponent of 0.35 was observed for the dependence of Rg on N for early collapsed intermediates [62]. On the other hand, a scaling exponent of 0.46 has been reported [63] for the chain-length dependence of the R_g of the U state in refolding conditions.

The collapsed globule (U_C) has hydrophobic patches

From previous millisecond mixing experiments, it was known that the kinetic MG populated at 1 ms after the initiation of folding contains hydrophobic patches that can bind ANS [45]. In order to determine the time scale of formation of these hydrophobic patches, the refolding of MNEI was carried out using microsecond mixing by monitoring the fluorescence of ANS. It was seen that ANS binding and its consequent increase in fluorescence were completed within the 37-μs burst phase (Fig. 4a). Hence, the hydrophobic patches capable of binding ANS were already formed within the mixing dead time of 37 μs. The ANS fluorescence then decreased at a rate slower than the rate of hyperfast decrease in intrinsic tryptophan fluorescence. This ultrafast phase decrease in ANS fluorescence had a time constant of 250 μs. The rate of the ultrafast decrease in ANS fluorescence was found to be independent of ANS concentration (Fig. S6), indicating that ANS did not modulate the kinetics of the ultrafast phase and that the observed change in the fluorescence of ANS was not limited by the amount of ANS used.

There are two possible explanations for the ultrafast decrease in ANS fluorescence. The first explanation is that the rate of ultrafast decrease represents the rate of dissociation of ANS from the intermediate (I_{VE}) formed at the end of the hyperfast phase of folding from U_C. ANS would dissociate from I_{VE} because it is less tightly bound to it than U_C. This explanation is unlikely because the ultrafast rate of decrease in ANS fluorescence has a significant dependence on GdnHCl concentration. It decreases from 6600 s^{-1} in 0.6 M GdnHCl to 4000 s^{-1} in 0.8 M GdnHCl, while the viscosity of the solution increases by only 1%.

The second possible explanation is that the ultrafast decrease in ANS fluorescence represents the transition of I_{VE} to a later intermediate from which it dissociates extremely rapidly. This explanation is more likely as the ultrafast rate decreases significantly with an increase in GdnHCl concentration (Fig. 4b), as expected for a folding process. The dissociation of ANS from some regions of the folding chain would occur as those parts of the chain become desolvated, resulting in the expulsion of water along with ANS. The observed rate constants for ANS-monitored refolding in the millisecond-to-second time domain, obtained upon stopped-flow mixing, were found to be comparable to those measured in previous studies [45,55].

IAEDANS moiety attached to C42 showed an increase in fluorescence within 37 μs

The refolding of MNEI was also monitored by probing the fluorescence of an IAEDANS moiety attached to the C42 thiol using both stopped-flow mixing and continuous-flow mixing. The fluorescence of IAEDANS is environment sensitive and was found to be higher for the N state than for the U state, which was expected, since C42 is buried at the interface of the sole α helix and the five β strands (Fig. 1) in the N state, while it is exposed to aqueous solvent in the U state. The equilibrium unfolding transition of MNEI showed a sigmoidal decrease in IAEDANS fluorescence, with an increase in GdnHCl

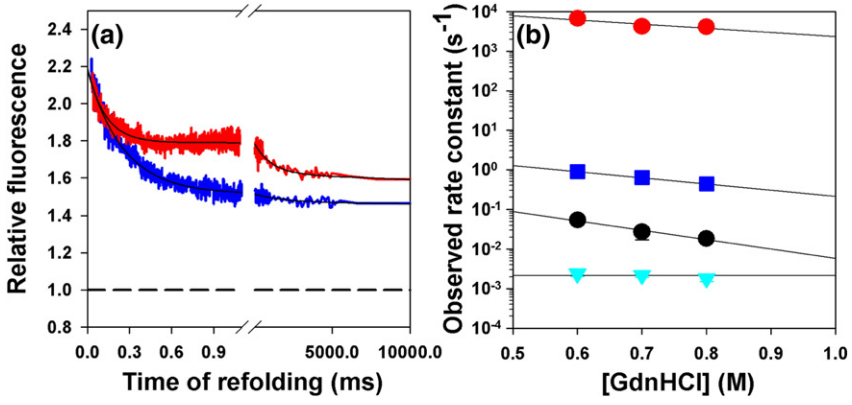

Fig. 4. ANS fluorescence monitored refolding kinetics of MNEI. (a) Representative kinetic traces of refolding in 0.6 (red) and in 0.8 (blue) M GdnHCl. The sub-millisecond data before the *x*-axis break were obtained from continuous-flow mixing, and the data from 6 ms onwards were obtained using stopped-flow mixing. The signal of the U protein in 4 M GdnHCl is shown as a dashed black line (b) The observed rate constants of refolding are plotted against GdnHCl concentration, ●, ultrafast phase; ■, fast phase; •, slow phase; ▼, very slow phase. The error bars, mostly hidden under the symbols, represent the spreads in the data from at least two repetitions of the experiments.

concentration (Fig. 5b). When the refolding kinetics of MNEI was monitored by the measurement of IAEDANS fluorescence after stopped-flow mixing, the fluorescence was observed to increase in a burst phase that was completed in the mixing dead time of 6.2 ms (Fig. 5a). In fact, this initial increase in the IAEDANS fluorescence occurred within the dead time of the microsecond mixing experiment itself, that is, within 37 μs (Fig. 5a). This result corroborated the observation that U_C had already formed hydrophobic patches that could bind ANS within 37 μs. It appeared that the region around C42 formed a hydrophobic cluster during the 37-μs burst phase, in which the IAEDANS moiety became buried, resulting in the enhancement of its fluorescence. After the initial increase in the 37-μs burst phase, the IAEDANS fluorescence remained constant for a few milliseconds, increasing again only when the kinetic MG folds further to the N state. This raises the possibility that the hydrophobic cluster that buries the IAEDANS moiety during the 37-μs burst phase might be native like, persisting during folding to the N state.

Discussion

The sub-millisecond folding reaction of MNEI was studied using multiple probes, and at least three kinetic phases could be detected during the first millisecond of folding. The initial collapse transition was found to be over within the 37-μs mixing dead time of the continuous-flow mixer. The product of the initial collapse reaction, U_C, is a collapsed globule having hydrophobic patches that are capable of binding ANS and having its tryptophan in a nonnative conformation. The subsequent dynamics that takes place in the collapsed globule represents the structural transitions that result in the formation of a kinetic MG at a few milliseconds of folding, from which structure formation proceeds along multiple parallel pathways.

MNEI undergoes polymer-like compaction

The observation that the collapse of the polypeptide chain is complete within 37 μs of the initiation of refolding, as seen by the burst-phase increase in FRET efficiency for all the 3 distances probed (Fig. 3), suggests that the initial polypeptide chain collapse reaction occurs with a time constant shorter than ~10 μs. For many other proteins too, the collapse transition was found to be over within the mixing dead time of the microsecond mixing experiment [15,16,19,37]. An upper limit of 1 μs was proposed for the collapse transition in proteins from the measurements of diffusion-limited contact formation in the U state of cytochrome *c* [58]. Hence,

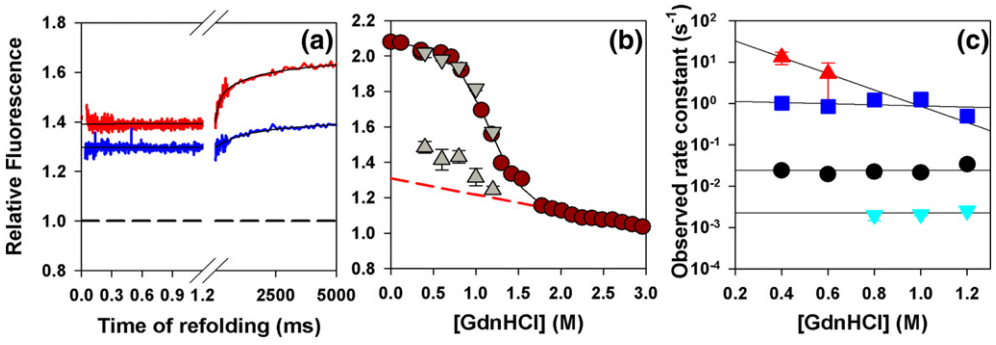

Fig. 5. Refolding of Cys42-IAEDANS. The fluorescence of the IAEDANS moiety was monitored at 470 nm upon excitation at 375 nm. (a) Representative kinetic traces at 0.6 M GdnHCl (red) and 1.0 M GdnHCl (blue). The sub-millisecond data before the *x*-axis break were obtained using continuous-flow mixing, and the data from 6 ms onwards were obtained using stopped-flow mixing. The signals are normalized to the signal of the U protein in 4 M GdnHCl (dashed black line). (b) Comparison of the equilibrium and kinetic amplitudes of the refolding of Cys42-IAEDANS; ●, the equilibrium unfolding transition; ▲, extrapolated $t = 0$ signals of the stopped-flow kinetic traces; ▼, $t = \infty$ signal of the stopped-flow kinetic traces. The solid black line through the equilibrium unfolding data is fit to a two-state, N↔U, unfolding model, which yielded a value for ΔG_u of 3.5 kcal/mol. The dashed red line represents the extrapolated U protein baseline. (c) The rate constants of the four observable phases of the refolding of C42-IAEDANS at different GdnHCl concentrations:▲, very fast phase; ■, fast phase; ●, slow phase; ▼, very slow phase. The solid black lines through the data points are linear regression fits. The error bars, mostly hidden under the symbols, represent the spreads obtained from at least two repetitions of the experiments.

the actual time scale of collapse is likely to be much faster than 10 μs in the case of MNEI. In the case of BBL, the time scale of polypeptide chain collapse had been measured by temperature-jump experiments to be around 60 ns at 305 K [22]. For cold-shock protein (Csp*Tm*), the global chain reconfiguration time, an equilibrium property which serves as an approximate upper limit for the collapse time, was found to be 50 ns from single-molecule FRET measurements [23].

The pre-exponential factor in the Arrhenius rate expression indicates the folding rate constant in the absence of a barrier. For the folding of the λ_{6-85} repressor, this was estimated to be 0.5–1 μs [64], and for BBL, it was estimated to be 1.3 μs at 333 K [65]. Indeed, the diffusion-limited folding speed limit, in the absence of a barrier, has been suggested to be N_R/100 μs, where N_R is the number of residues [66]. For a 100-residue protein, the time scale of diffusion-limited folding is 1 μs. A similar speed limit has been obtained from a theoretical analysis of kinetic data on fast-folding proteins [67]. The current study suggests that the collapse transition of MNEI, which occurs with a time constant of less than 10 μs, is slowed down by a barrier of only ~ $2k_BT$, compared to how fast it might occur in the absence of any barrier. Such a small barrier could conceivably be traversed by thermal fluctuations, and it is possible that the initial collapse transition might effectively occur through a continuum of states. However, it should be noted that the only definitive way to determine whether a protein folding or unfolding transition occurs in a continuous manner or not would be to examine the evolution of population distribution of molecules at different times during the process [57]. It should also be noted that neither from the results of the previous experiments [16,45] nor from the results of the current study was it possible to determine whether all MNEI molecules have undergone collapse and whether the collapsed molecules have all contracted to the same extent.

In the current study, the increases in FRET efficiency were different for the different donor–acceptor pairs, suggesting that the different segments contract to different extents, with the longer segment contracting more (Fig. 3 and Table S1). The value of R_g can be determined with confidence for the whole protein only in the U state, but not in U_C (see Results). Hence, it is difficult to determine how accurate are the extents to which the three segments of the protein appear to have contracted in U_C. The different extents, in the range of 15–47% (Table S1), to which the three different distances appear to have contracted could either be real and due to the structure present in U_C or be an artifact due to uncertainty in the determination of R_g for U_C (see Results). In a previous study, the extent of initial collapse was determined by SAXS to be 30% collapse [16]. For several other proteins, SAXS measurements showed that R_g changes by 40–50% during the entire folding reaction and by 20–30% during the initial collapse transition [68]. On the other hand, single-molecule FRET measurements indicated that the initial extent of contraction upon collapse is 30–40% [68].

It should be noted that FRET is more biased towards shorter distances, whereas scattering intensity is biased towards longer distances. For some proteins, SAXS measurements were unable to detect any collapse having occurred during the formation of the kinetic MG [69–71], presumably because the fractional contraction was too small to be measured by SAXS. In FRET measurements, specific distances are measured, very often just one [32,35,72,73], and it is possible that even when one segment of the protein undergoes contraction, which can be measured by FRET, the overall dimensions of the protein do not decrease sufficiently to be measured by SAXS. It is therefore important to carry out multisite FRET to establish the extent of volume compaction during the early collapse transition and to compare these measurements with SAXS measurements.

Specificity of initial collapse reaction of MNEI

Multisite FRET has been used to characterize the dimensions of the kinetic MGs of several proteins [29,31,41]. In earlier studies, the collapse transition was said to be non-specific if the FRET efficiencies in the kinetic MG at low denaturant (refolding) conditions could be predicted by extrapolation of the FRET efficiencies in the U state at high denaturant (unfolding) conditions [29,31,44]. The collapsed state would then correspond to the U state in refolding conditions. The collapse transition was said to be specific if the FRET efficiencies for at least a few segments of the protein were more than that expected from such extrapolation in the U protein at the lower denaturant concentration [44].

In the previous study [45], it was seen that two of the segments (W4-C42 and W4-C97) underwent compaction to an extent that was more than that expected for the U state in refolding conditions and that the only sequence segment W4-C29, which spans the sole helix, underwent a solvent-induced compaction that could be predicted by the behavior of the U state at the high denaturant concentrations. In the current study, it has been shown that the initial contraction is complete within the first 37 μs of folding in U_C itself. The sequence segments that contract more than expected might be doing so because they form some structure. Some of this structure in U_C appears to be nonnative, as indicated by the observation that W4 has become transiently buried presumably in a local hydrophobic cluster. From the current study, it is not possible to say whether the initial compaction in MNEI was brought

about by specific interactions that are also present in the final N state or by non-specific interactions similar to a polymer collapse. Several observations, including the time scale of the initial chain collapse (<10 μs), the nonnative burial of W4, the correlation between the extent of contraction during the U-to-U_C transition and the length of the sequence segment, the gradual change in the size of U_C with denaturant concentration, and the absence of the sole helix [45] suggest that the burst-phase product at 37 μs of refolding is a collapsed unfolded state (U_C) and not an intermediate with specific structure. Non-specific, polymer-like compaction prior to the folding transition has been seen for several proteins [4,20,27,29,31,33,40,41,43,44,74]. It has been suggested that only when the folding temperature is close to the collapse temperature will the initial collapse transition result in the formation of specific structure [75].

The initially collapsed globule of MNEI has solvent-exposed hydrophobic patches

The observation that the fluorescence of the extrinsic fluorophore ANS increases in the 37-μs burst phase (Fig. 4) suggests that the burst-phase product U_C has hydrophobic patches that can bind ANS. It should be noted that while the binding of ANS to hydrophobic patches, which were formed in the collapsed globules populated during the first millisecond of folding, has been interpreted to mean that the collapsed globule has specific structure [37], a non-specific collapse driven by hydrophobic interactions can also lead to an increase in ANS fluorescence [29]. The burst-phase increase in the fluorescence of W4 (Fig. 2) and of IAEDANS moiety (Fig. 5) attached to the protein indicates that the W4 and C42 regions of the protein are both parts of the regions that form these hydrophobic patches. Interestingly, the hydrophobic cluster that buries W4 seems to be nonnative, since it dissolves in the hyperfast phase as seen by the decrease in fluorescence of W4 (Fig. 2). On the other hand, the hydrophobic cluster around C42 may be native like, as it does not dissolve but is retained in the kinetic MG at a few milliseconds of folding (Fig. 5a). Thereafter, the cluster is further consolidated during the main folding reactions; IAEDANS fluorescence is further enhanced as the kinetic MG folds (Fig. 5a).

Some studies indicate that the initial collapse transition is due to hydrophobic interactions between the side chains [4,22,76]. In the current study, the observation that the formation of hydrophobic patches and compaction of the polypeptide chain are complete within the 37-μs burst phase suggests that the collapse transition in MNEI might be due to hydrophobic side-chain-mediated interactions. In a theoretical study [77], using a heteropolymer having hydrophobic and hydrophilic monomers similar to proteins, it was proposed that the hydrophobic side-chain-driven compaction results in the formation of minimum energy compact (MEC) states and that proteins are able to fold on biologically relevant time scales due to the formation of these MECs during the first millisecond of folding [77]. The earliest compact state U_C observed in this study might qualify as a MEC.

In the current study of the folding of MNEI, hydrophobic patches were seen to form within the 37-μs burst phase; while in an earlier study of MNEI [16], they were observed to form with a time constant of 19 ± 1 ms, when the folding was started from MNEI unfolded at pH 12. There could be two reasons for this difference: (1) The U states at high pH and at high GdnHCl might be different, and they might fold by traversing different routes on the multidimensional energy landscape. An analogous difference was observed for λ_{6-85} repressor protein for folding, which was induced by a temperature jump and by microfluidic mixing, and had been attributed to differences in the U states populated at high temperature and high denaturants [78]. (2) A less likely explanation for the difference in the rates observed is the slight difference in the proteins used in the two studies. The variant of MNEI used in the earlier pH-jump-induced folding study lacks the linker dipeptide (glycine-phenylalanine) and had the sole cysteine mutated to a serine. In the current study, it is shown that the C42 region undergoes a major structural transition during the 37-μs burst phase, as shown by the refolding experiment using the fluorescence of the IAEDANS moiety attached to C42as the probe (Fig. 5).

The tryptophan microenvironment changes during the sub-millisecond folding of MNEI

Most folding studies carried out in the sub-millisecond time domain have used tryptophan fluorescence as the probe [79–81]. The fluorescence of tryptophan can change due to a change in its microenvironment, due to quenching by different groups in the protein, due to a change in solvation, or due to FRET with an acceptor moiety attached to the protein. In the current study, the observation of a burst-phase increase in tryptophan fluorescence and a blue shift in its emission maximum (Fig. 2) suggests the transient formation of nonnative interactions, since the fluorescence of W4 shows a consequent decrease in a hyperfast phase as opposed to an expected increase during folding. Similar increases in tryptophan fluorescence within a few μs of the initiation of folding have been observed for RNaseH [54], cytochrome *c*, apomyoglobin and lysozyme [19], and acyl-CoA binding protein [82]. In the current study, even though a hyperfast decrease in tryptophan fluorescence was observed for both TNB-labeled and unlabeled proteins (Fig. 3), the

FRET efficiency did not change during this phase, which suggests that the decrease in tryptophan fluorescence is due to a change in local environment and that the dimensions of the polypeptide chain remain unchanged during the hyperfast phase. A similar change in tryptophan fluorescence without a change in the dimensions of the protein was also observed during the sub-millisecond folding of protein L [43]. Several sub-millisecond folding studies have tried to interpret a decrease in tryptophan fluorescence in the presence of a FRET acceptor as a collapse transition [19,35,42]. If tryptophan fluorescence is measured only in the presence of a FRET acceptor, and that is seen to decrease, the decrease may not be because of FRET but because the quantum yield of the donor tryptophan itself decreases. The observation of a change in tryptophan fluorescence in the absence of a FRET acceptor without any change in the overall dimensions of the protein in the case of protein L and MNEI, emphasizes the need to interpret the kinetics monitored by tryptophan fluorescence more conservatively.

Sub-millisecond folding of MNEI occurs in multiple steps

The sub-millisecond dynamics of MNEI monitored by different probes indicates that the kinetic MG observed at a few ms of folding reaction is the product of three different events happening within the sub-millisecond time domain. The results of the current study are summarized in Fig. 6. The scheme proposed is the simplest scheme and does not negate the possibility of more complex parallel pathways predicted for the early folding events. The compaction event due to the collapse transition is over within the mixing dead time, and U_C has hydrophobic patches that can bind ANS and W4 in a nonnative conformation. U_C also has the IAEDANS adduct on C42, buried in a hydrophobic cluster that might be native like because the burial of the IAEDANS moiety persists right up to and in the N state. On the other hand, the nonnative structure around W4 dissolves in a hyperfast phase, with a time constant of 50 μs, which results in the formation of a very early intermediate (I_{VE}). I_{VE} undergoes an ultrafast decrease in ANS fluorescence, which would be due to the expulsion of water from the protein, resulting in the formation of kinetic MG. It is likely that this dehydration of the chain facilitates the formation of backbone hydrogen bonds and the initiation of formation of secondary structure in the kinetic MG.

The funnel-shaped energy landscape envisaged for proteins [83–85] suggests that the folding reaction is more heterogeneous at the earliest stages of folding. Conformational heterogeneity is lost incrementally as the folding reaction proceeds [86]. In previous studies, multiple kinetic phases were observed during the sub-millisecond folding of protein L [43], barstar [20], and cytochrome *c* [19,35,87]. The lack of cooperativity also suggests that the folding reaction on the sub-millisecond time scale is not limited by a large free energy barrier; instead, it occurs in multiple steps, each having a marginal barrier ($<3\ k_BT$). The activation energies obtained for the dynamics of different segments of MNEI were $\sim 9\ k_BT$ (5.2 kcal/mol, 6.7 kcal/mol, and 5.2 kcal/mol for Cys29-TNB, Cys42-TNB, and Cys97-TNB, respectively) (Fig. S3d). The viscosity of water has an Arrhenius-like dependence on temperature, and the change in viscosity due to an increase in temperature contributes 7 k_BT to the barrier height [72]. Thus, only marginal barriers of around 2 k_BT separate the different conformational sub-states in the collapsed globule.

In an equilibrium model for the formation of a productive MG of barstar [27,74], the pH unfolded

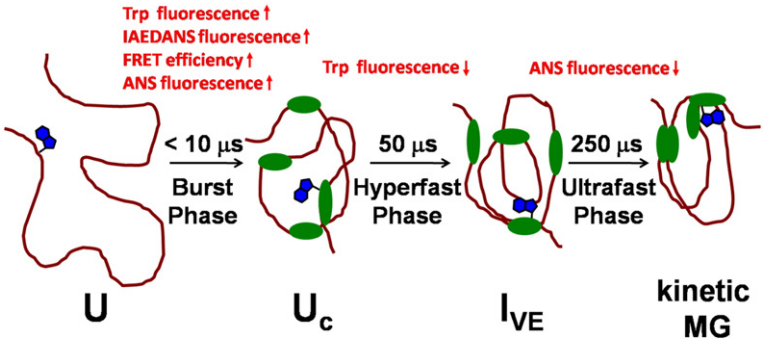

Fig. 6. Cartoon diagram showing the sequence of events happening during the first 1 ms of folding. The unfolded protein undergoes burst-phase collapse within 10 μs of initiation of folding. The initial chain collapse is accompanied by differential increases in the FRET efficiencies of different D–A pairs, an increase in the fluorescence of W4 (blue residue) and of an IAEDANS moiety attached to C42, and an increase in fluorescence of ANS. The collapsed globule undergoes a hyperfast phase decrease in tryptophan fluorescence and forms a very early intermediate, I_{VE}. Desolvation of some regions of I_{VE} results in an ultrafast decrease in ANS fluorescence, leading to the formation of a kinetic MG that then proceeds to fold to the N state. The green ovals represent the hydrophobic patches.

form of barstar was shown to undergo folding through multiple equilibrium intermediates in a noncooperative manner, upon the addition of salt to screen electrostatic repulsion in the chain. Kinetic studies showed that these equilibrium intermediates were on pathway to the N state [27]. A sub-millisecond kinetic study of the folding of barstar showed that a collapse transition precedes the first structure formation step, both occurring within a millisecond of the initiation of folding [20]. The sub-millisecond structure formation reaction of barstar was shown to be barrierless, based on the observation of the rate being independent of denaturant concentration and temperature [20]. The observation that the sub-millisecond folding reactions of many other proteins also have negligible dependences on denaturant concentration [35,82,88,89] suggests that these early folding transitions may, in general, not be slowed down by sizable free energy barriers.

Dynamics within the collapsed globule

The initial collapse transition of MNEI is over within the 37-μs burst phase (Fig. 3). The two observable structural transitions, namely the hyperfast decrease in tryptophan fluorescence (Figs. 2, 3) and the ultrafast decrease in ANS fluorescence (Fig. 4), represent the structural rearrangements that prime the subsequent folding reaction. The dimensions of the protein remain unchanged during these two structural transitions. Sub-millisecond dynamics without a change in the overall size of the protein after the initial chain collapse was observed for DHFR [18], protein L [43], MNEI [16], apomyoglobin [15], and ribonuclease A [37]. The sub-millisecond dynamics of cytochrome *c*, apomyoglobin, and lysozyme observed with tryptophan fluorescence as the probe were interpreted as the formation of native tertiary contacts [19]. However, tryptophan fluorescence can also change due to a change in its local environment and hence may not be indicative of the formation of tertiary contacts.

The current study shows that the nonnative interactions formed during the initial collapse transition are rearranged to enable the protein to fold to its native structure. These dynamics within the collapsed globule might be the defining features of sequences that can undergo folding. It was argued that the initial collapse transition may not be the signature of a sequence that can fold successfully [90]: for several proteins, the collapse transition can be mimicked by non-foldable analogs of the same proteins [90–93]. This again hints at the non-specific, polymer-like nature of the initial collapse transition. It seems that the foldability of a sequence comes into play only after the initial collapse transition, when the collapsed polypeptide chain undergoes rearrangements dictated by the chemistry of the sequence, which prime the actual folding reaction.

The N state of MNEI expands upon addition of denaturant

While this study has revealed much about the microsecond folding events in the initially collapsed globule of MNEI and their dependence on low concentrations of GdnHCl, it has also revealed interesting information on how low concentrations of GdnHCl affect the N state of the protein. The fluorescence of the buried W4 in native MNEI has a steep dependence on GdnHCl concentration in the range from 0 to 1.4 M (Fig. 2c): it increases by 20% while that of NATA increases only by 7% (data not shown). A simple explanation for this observation is that fluorescence in the N state is quenched by the local structure, and the addition of denaturant causes the N state to expand slightly, thus resulting in the quenching being released and in increased fluorescence. Indeed, the N state of MNEI had been shown in previous FRET-based studies to expand upon the addition of denaturant [45,89,94]. Similar denaturant-induced expansion of the N state has also been observed for barstar [95] and for the SH3 domains of PI3 kinase [29] and α-spectrin [96]. It is possible that this may be a general property of proteins, which is difficult to detect by most conventional probes.

Conclusion

The sub-millisecond folding reaction of MNEI from the GdnHCl-unfolded state has been studied using multiple fluorescence-based probes. The compaction of the polypeptide chain is shown to be over within the mixing dead time of 37 μs. The resultant collapsed globule has the sole tryptophan buried in a nonnative conformation and has already formed hydrophobic patches that can bind the dye ANS. A hyperfast decrease in tryptophan fluorescence occurs with a time constant of 50 μs, and an ultrafast decrease in the ANS fluorescence occurs with a time constant of 250 μs. All these transitions are over within the first millisecond of folding, when the specific, native-like secondary structure is yet to form. The upper limit for chain collapse is estimated to be 10 μs. The presence of multiple kinetic phases reveals the noncooperative nature of early sub-millisecond folding. The sub-millisecond kinetic phases likely represent the structural rearrangements that help in breaking nonnative interactions formed due to the initial non-specific collapse and the desolvation of some parts of the collapsed polypeptide chain, which helps in preparing it for the actual folding transition.

Materials and Methods

Buffers and reagents

All the chemicals used in the current study were of high purity grade and were obtained from Sigma. Ultra-pure GdnHCl was obtained from United States Biochemicals. The native buffer used was 50 mM sodium phosphate at pH 7 containing 250 μM EDTA and 1 mM DTT. DTT was not added in the experiments with the TNB-labeled proteins since it caused the detachment of the label. Unfolding buffer was prepared by adding 4 M GdnHCl to the native buffer.

Protein purification

The variants of MNEI were purified according to the protocol described previously [55]. Cys42 (wt MNEI) had cysteine at residue position 42, while Cys29 and Cys97 had the cysteine at residue position 29 and 97, respectively. The purity and mass of each protein were verified by electrospray ionization mass spectrometry (ESI-MS), and the proteins were found to be more than 95% pure. The concentration of the protein was determined using the molar extinction coefficient of 14,600 M^{-1} cm^{-1} [55]. In the case of TNB-labeled proteins, the contribution of the TNB label to the absorbance at 280 nm was corrected as described earlier [31].

TNB and IAEDANS labeling of MNEI

The labeling of MNEI with IAEDANS and TNB was carried out as described previously [57,97]. In the case of the TNB-labeled protein, the extent of labeling was checked by ESI-MS, and the molecular mass of the protein was found to increase by 196 Da, which corresponded to the mass of the TNB moiety. The extent of labeling was found to be >95%. In the case of the IAEDANS-labeled protein, the extent of labeling was checked both by absorbance measurement and ESI-MS and was found to be >90%. The mass of the protein increased by 306 Da upon the addition of the IAEDANS moiety.

Equilibrium unfolding studies

Equilibrium unfolding experiments, in which the fluorescence of the IAEDANS moiety attached to C42 was monitored, were carried out using the stopped-flow module (SFM-4) from Biologic. The sample was excited at 375 nm, and the fluorescence emission was collected at 470 nm using a 470 ± 10 nm band pass filter (Asahi Spectra). The protein was incubated with different concentrations of GdnHCl for 6 h at room temperature (25 °C) before the fluorescence was measured.

The SFM-4 module was also used for equilibrium unfolding experiments in which tryptophan fluorescence was used as the probe. The sample was excited at 295 nm, and the fluorescence was collected at 340 nm using a 340 ± 10 nm band pass filter (Asahi Spectra). The protein concentration used was 10 μM, and the path length of the cuvette was 1 cm.

Millisecond kinetic refolding studies

All the millisecond kinetic refolding experiments were carried out on the SFM-4 stopped-flow module. A dead time of 1.8 ms was achieved by using a cuvette with a path length of 0.8 mm and a flow rate of 5 mL/s. For refolding experiments in which intrinsic tryptophan fluorescence was monitored, the sample was excited at 295 nm, and the fluorescence was collected at either 360 nm or 340 nm, using a 360 ± 10 nm or a 340 ± 10 nm band pass filter (Asahi Spectra).

For refolding experiments in which ANS fluorescence and IAEDANS fluorescence were monitored using the SFM-4 module from Biologic, a dead time of 6.2 ms was achieved using a cuvette of path length 1.5 mm and a flow rate of 5 mL/s. The sample was excited at 375 nm, and the fluorescence was collected at 470 nm using a 470 ± 10 nm band pass filter (Asahi Spectra). The data was collected using the MOS-450 acquisition system (Biologic).

Microsecond mixing refolding experiments

The microsecond mixing experiments were carried out using a custom-built, continuous-flow mixing setup. The design of the continuous-flow mixing setup and the experimental procedure for microsecond mixing experiments are described in the Supplementary Data (Fig. S1). The dead time was determined to be 37 ± 5 μs by carrying out experiments in which the kinetics of quenching of the fluorescence of NATA by *N*-bromosuccinimide (Fig. S2) was monitored.

Fitting equilibrium unfolding curves

The equilibrium unfolding transition was fit to a two-state model to obtain the free energy of unfolding in water and its dependence on denaturant concentration (*m* value) [98].

FRET efficiency calculation

The FRET efficiency (E) was calculated from the fluorescence values of the unlabeled and TNB-labeled proteins using Eq. (1).

$$E = 1 - \frac{F_{DA}}{F_D} \tag{1}$$

F_{DA} is the fluorescence of the donor in the presence of acceptor (tryptophan fluorescence of the TNB-labeled protein) and F_D is the donor-only fluorescence (tryptophan fluorescence of the unlabeled protein).

For the U state, the value of R_0 had been determined earlier [57] using Eq. (2):

$$R_0 = 0.211 \left(Q_D\ J\kappa^2\eta^{-4}\right)^{1/6} \tag{2}$$

Q_D is the quantum yield of the donor, J is the overlap integral that signifies the spectral overlap between the donor's emission spectrum and the acceptor's absorption spectrum, κ^2 is the orientation factor, and η is the refractive index of the medium used. A value of 2/3 for κ^2 was used, which assumes the free rotation of the donor and acceptor moieties.

Acknowledgments

We thank Osman Bilsel and Sagar Kathuria for providing us with the design of the quartz micro-fluidic chip used in the continuous-flow setup and for e-mail discussions on its usage, Satoshi Takahashi for suggesting the epi-fluorescence mode of imaging of the mixing chip, and Manoj Mathew and Shree Krishnamurthy for helping us with the optical setup. We thank Gilad Haran for providing us with the program to calculate RMS distance and R_g from the FRET efficiency using the Gaussian chain model and the mechanical work shop at NCBS for making several opto-mechanical parts used in the continuous-flow setup. We thank G. Krishnamoorthy and members of our laboratory for discussions and comments on the manuscript; and Devarajan Thirumalai, Govardhan Reddy, and Madan Rao for useful discussions.

This work was funded by the Tata Institute of Fundamental Research and by the Department of Science and Technology, Government of India. J.B.U. is a recipient of a JC Bose National Fellowship from the Government of India.

Appendix A. Supplementary Data

Supplementary data to this article can be found online at http://dx.doi.org/10.1016/j.jmb.2016.06.015.

Received 16 February 2016;
Received in revised form 17 June 2016;
Accepted 19 June 2016
Available online 28 June 2016

Keywords:
monellin;
collapse;
sub-millisecond folding;
microsecond mixing;
multi-site FRET

Abbreviations used:
MG, molten globule; N state, native state; U, unfolded state; MNEI, monellin; SAXS, small angle X-ray scattering; ANS, 1-anilino napthalene8-sulfonate; TNB, thionitrobenzoate; NATA, *N*-acetyl-L-tryptophanamide; I_{VE}, intermediate; MEC, minimum energy compact; ESI-MS, electrospray ionization mass spectrometry.

References

[1] K. Kuwajima, Y. Hiraoka, M. Ikeguchi, S. Sugai, Comparison of the transient folding intermediates in lysozyme and alpha-lactalbumin, Biochemistry. 24 (1985) 874–881, http://dx.doi.org/10.1021/bi00325a010.

[2] K. Kuwajima, The molten globule state as a clue for understanding the folding and cooperativity of globular-protein structure, Proteins Struct. Funct. Bioinf. 6 (1989) 87–103, http://dx.doi.org/10.1002/prot.340060202.

[3] J.B. Udgaonkar, Polypeptide chain collapse and protein folding, Arch. Biochem. Biophys. 531 (2013) 24–33, http://dx.doi.org/10.1016/j.abb.2012.10.003.

[4] V.R. Agashe, M.C.R. Shastry, J.B. Udgaonkar, Initial hydrophobic collapse in the folding of barstar, Nature. 377 (1995) 754–757, http://dx.doi.org/10.1038/377754a0.

[5] P.A. Jennings, P.E. Wright, Formation of a molten globule intermediate early in the kinetic folding pathway of apomyoglobin, Science 80. (262) (1993) 892–896, http://dx.doi.org/10.2307/2882624.

[6] K. Kuwajima, G.V. Semisotnov, A.V. Finkelstein, S. Sugai, O.B. Ptitsyn, Secondary structure of globular proteins at the early and the final stages in protein folding, FEBS Lett. 334 (1993) 265–268, http://dx.doi.org/10.1016/0014-5793(93)80691-M.

[7] Z.Y. Peng, P.S. Kim, A protein dissection study of a molten globule, Biochemistry. 33 (1994) 2136–2141.

[8] K.H. Mok, T. Nagashima, I.J. Day, P.J. Hore, C.M. Dobson, Multiple subsets of side-chain packing in partially folded states of α-lactalbumins, Proc. Natl. Acad. Sci. U. S. A. 102 (2005) 8899–8904.

[9] L. Pradeep, J.B. Udgaonkar, Differential salt-induced stabilization of structure in the initial folding intermediate ensemble of barstar, J. Mol. Biol. 324 (2002) 331–347, http://dx.doi.org/10.1016/S0022-2836(02)01068-9.

[10] L. Pradeep, J.B. Udgaonkar, Osmolytes induce structure in an early intermediate on the folding pathway of barstar, J. Biol. Chem. 279 (2004) 40,303–40,313, http://dx.doi.org/10.1074/jbc.M406323200.

[11] T. Kiefhaber, R.L. Baldwin, Intrinsic stability of individual α helices modulates structure and stability of the apomyoglobulin molten globule form, J. Mol. Biol. 252 (1995) 122–132, http://dx.doi.org/10.1006/jmbi.1995.0479.

[12] D. Hamada, S. Segawa, Y. Goto, Non-native [alpha]-helical intermediate in the refolding of [beta]-lactoglobulin, a predominantly [beta]-sheet protein, Nat. Struct. Mol. Biol. 3 (1996) 868–873, http://dx.doi.org/10.1038/nsb1096-868.

[13] D.M. Rothwarf, H.A. Scheraga, Role of non-native aromatic and hydrophobic interactions in the folding of hen egg white lysozyme, Biochemistry. 35 (1996) 13,797–13,807.

[14] S. Takahashi, S.-R. Yeh, T.K. Das, C.-K. Chan, D.S. Gottfried, D.L. Rousseau, Folding of cytochrome *c* initiated by submillisecond mixing, Nat. Struct. Mol. Biol. 4 (1997) 44–50, http://dx.doi.org/10.1038/nsb0197-44.

[15] T. Uzawa, S. Akiyama, T. Kimura, S. Takahashi, K. Ishimori, I. Morishima, et al., Collapse and search dynamics of apomyoglobin folding revealed by submillisecond observations of alpha-helical content and compactness, Proc. Natl. Acad. Sci. U. S. A. 101 (2003) 1171–1176, http://dx.doi.org/10.1073/pnas.0305376101.

[16] T. Kimura, T. Uzawa, K. Ishimori, I. Morishima, S. Takahashi, T. Konno, et al., Specific collapse followed by slow hydrogen-bond formation of β-sheet in the folding of single-chain monellin, Proc. Natl. Acad. Sci. U. S. A. 102 (2005) 2748–2753, http://dx.doi.org/10.1073/pnas.0407982102.

[17] A. Hoffmann, A. Kane, D. Nettels, D.E. Hertzog, P. Baumgärtel, J. Lengefeld, et al., Mapping protein collapse with single-molecule fluorescence and kinetic synchrotron radiation circular dichroism spectroscopy, Proc. Natl. Acad.

Sci. U. S. A. 104 (2007) 105–110, http://dx.doi.org/10.1073/pnas.0604353104.
[18] M. Arai, E. Kondrashkina, C. Kayatekin, C.R. Matthews, M. Iwakura, O. Bilsel, Microsecond hydrophobic collapse in the folding of *Escherichia coli* dihydrofolate reductase, an alpha/beta-type protein, J. Mol. Biol. 368 (2007) 219–229, http://dx.doi.org/10.1016/j.jmb.2007.01.085.
[19] L.J. Lapidus, S. Yao, K.S. McGarrity, D.E. Hertzog, E. Tubman, O. Bakajin, Protein hydrophobic collapse and early folding steps observed in a microfluidic mixer, Biophys. J. 93 (2007) 218–224, http://dx.doi.org/10.1529/biophysj.106.103077.
[20] K.K. Sinha, J.B. Udgaonkar, Barrierless evolution of structure during the submillisecond refolding reaction of a small protein, Proc. Natl. Acad. Sci. U. S. A. 105 (2008) 7998–8003.
[21] Y. Wu, E. Kondrashkina, C. Kayatekin, C.R. Matthews, O. Bilsel, Microsecond acquisition of heterogeneous structure in the folding of a TIM barrel protein, Proc. Natl. Acad. Sci. 105 (2008) 13,367–13,372, http://dx.doi.org/10.1073/pnas.0802788105.
[22] M. Sadqi, L.J. Lapidus, V. Munoz, How fast is protein hydrophobic collapse ? Proc. Natl. Acad. Sci. 100 (2003) 12,117–12,122.
[23] D. Nettels, I.V. Gopich, A. Hoffmann, B. Schuler, Ultrafast dynamics of protein collapse from single-molecule photon statistics, Proc. Natl. Acad. Sci. 104 (2007) 2655–2660, http://dx.doi.org/10.1073/pnas.0611093104.
[24] P.J. Flory, Principles of Polymer Chemistry, Configurational and frictional properties of the polymer molecule in dilute solution. Cornel University Press, Ithaca, NY 1953, pp. 610–654.
[25] P.G. De Gennes, Collapse of a polymer chain in poor solvents, J. Phys. Lett. 36 (1975) 55–57, http://dx.doi.org/10.1051/jphyslet:0197500360305500.
[26] A.R. Khokhlov, Statistical Physics of Macromolecules, Single macro molecule with volume interactions, AIP Press 1994, pp. 109–144 (http://books.google.co.in/books?id=HlTi_3Jy8WgC).
[27] B.R. Rami, J.B. Udgaonkar, Mechanism of formation of a productive molten globule form of barstar, Biochemistry. 41 (2002) 1710–1716, http://dx.doi.org/10.1021/bi0120300.
[28] V. Ratner, D. Amir, E. Kahana, E. Haas, Fast collapse but slow formation of secondary structure elements in the refolding transition of *E. coli* adenylate kinase, J. Mol. Biol. 352 (2005) 683–699, http://dx.doi.org/10.1016/j.jmb.2005.06.074.
[29] A. Dasgupta, J.B. Udgaonkar, Evidence for initial non-specific polypeptide chain collapse during the refolding of the SH3 domain of PI3 kinase, J. Mol. Biol. 403 (2010) 430–445, http://dx.doi.org/10.1016/j.jmb.2010.08.046.
[30] B. Schuler, E.A. Lipman, W.A. Eaton, Probing the free-energy surface for protein folding with single-molecule fluorescence spectroscopy, Nature. 419 (2002) 743–747, http://dx.doi.org/10.1038/nature01060.
[31] K.K. Sinha, J.B. Udgaonkar, Dependence of the size of the initially collapsed form during the refolding of barstar on denaturant concentration: evidence for a continuous transition, J. Mol. Biol. 353 (2005) 704–718, http://dx.doi.org/10.1016/j.jmb.2005.08.056.
[32] E. Sherman, G. Haran, Coil-globule transition in the denatured state of a small protein, Proc. Natl. Acad. Sci. U. S. A. 103 (2006) 11,539–11,543, http://dx.doi.org/10.1073/pnas.0601395103.
[33] K.M. Hamadani, S. Weiss, Nonequilibrium single molecule protein folding in a coaxial mixer, Biophys. J. 95 (2008) 352–365, http://dx.doi.org/10.1529/biophysj.107.127431.
[34] G. Ziv, G. Haran, Protein folding, protein collapse, and tanford's transfer model: lessons from single-molecule FRET, J. Am. Chem. Soc. 131 (2009) 2942–2947, http://dx.doi.org/10.1021/ja808305u.
[35] M.C.R. Shastry, H. Roder, Evidence for barrier-limited protein folding kinetics on the microsecond time scale, Nat. Struct. Mol. Biol. 5 (1998) 385–392, http://dx.doi.org/10.1038/nsb0598-385.
[36] J.G. Lyubovitsky, H.B. Gray, J.R. Winkler, Mapping the cytochrome *c* folding landscape, J. Am. Chem. Soc. 124 (2002) 5481–5485, http://dx.doi.org/10.1021/ja017399r.
[37] T. Kimura, S. Akiyama, T. Uzawa, K. Ishimori, I. Morishima, T. Fujisawa, et al., Specifically collapsed intermediate in the early stage of the folding of ribonuclease A, J. Mol. Biol. 350 (2005) 349–362, http://dx.doi.org/10.1016/j.jmb.2005.04.074.
[38] H.S. Chan, K.a. Dill, Origins of structure in globular proteins, Proc. Natl. Acad. Sci. 87 (1990) 6388–6392, http://dx.doi.org/10.1073/pnas.87.16.6388.
[39] S. Vaitheeswaran, J. Chen, D. Thirumalai, Hydrophobic and ionic interactions in bulk and confined water with implications for collapse and folding of proteins, J. Stat. Phys. 145 (2011) 276–292.
[40] E.a. Lipman, B. Schuler, O. Bakajin, W.a. Eaton, Single-molecule measurement of protein folding kinetics, Science 301 (2003) 1233–1235, http://dx.doi.org/10.1126/science.1085399.
[41] C. Magg, F.X. Schmid, Rapid collapse precedes the fast two-state folding of the cold shock protein, J. Mol. Biol. 335 (2004) 1309–1323, http://dx.doi.org/10.1016/j.jmb.2003.11.050.
[42] E. Welker, K. Maki, M.C.R. Shastry, D. Juminaga, R. Bhat, H.a. Scheraga, et al., Ultrarapid mixing experiments shed new light on the characteristics of the initial conformational ensemble during the folding of ribonuclease A, Proc. Natl. Acad. Sci. U. S. A. 101 (2004) 17,681–17,686, http://dx.doi.org/10.1073/pnas.0407999101.
[43] S.a. Waldauer, O. Bakajin, T. Ball, Y. Chen, S.J. Decamp, M. Kopka, et al., Ruggedness in the folding landscape of protein L, HFSP J. 2 (2008) 388–395, http://dx.doi.org/10.2976/1.3013702.
[44] K.K. Sinha, J.B. Udgaonkar, Dissecting the non-specific and specific components of the initial folding reaction of barstar by multi-site FRET measurements, J. Mol. Biol. 370 (2007) 385–405, http://dx.doi.org/10.1016/j.jmb.2007.04.061.
[45] R.R. Goluguri, J.B. Udgaonkar, Rise of the helix from a collapsed globule during the folding of monellin, Biochemistry (2015) http://dx.doi.org/10.1021/acs.biochem.5b00730.
[46] U. Nath, J.B. Udgaonkar, Folding of tryptophan mutants of barstar: evidence for an initial hydrophobic collapse on the folding pathway, Biochemistry. 36 (1997) 8602–8610, http://dx.doi.org/10.1021/bi970426z.
[47] H.J. Dyson, P.E. Wright, H.A. Scheraga, The role of hydrophobic interactions in initiation and propagation of protein folding, Proc. Natl. Acad. Sci. 103 (2006) 13,057–13,061.
[48] D.P. Teufel, C.M. Johnson, J.K. Lum, H. Neuweiler, Backbone-driven collapse in unfolded protein chains, J. Mol. Biol. 409 (2011) 250–262, http://dx.doi.org/10.1016/j.jmb.2011.03.066.
[49] A. Möglich, K. Joder, T. Kiefhaber, End-to-end distance distributions and intrachain diffusion constants in unfolded polypeptide chains indicate intramolecular hydrogen bond

formation, Proc. Natl. Acad. Sci. U. S. A. 103 (2006) 12,394–12,399, http://dx.doi.org/10.1073/pnas.0604748103.
[50] K. Chattopadhyay, E.L. Elson, C. Frieden, The kinetics of conformational fluctuations in an unfolded protein measured by fluorescence methods, Proc. Natl. Acad. Sci. U. S. A. 102 (2005) 2385–2389.
[51] H. Chen, E. Rhoades, J.S. Butler, S.N. Loh, W.W. Webb, Dynamics of equilibrium structural fluctuations of apomyoglobin measured by fluorescence correlation spectroscopy, Proc. Natl. Acad. Sci. 104 (2007) 10,459–10,464.
[52] S.a. Waldauer, O. Bakajin, L.J. Lapidus, Extremely slow intramolecular diffusion in unfolded protein L, Proc. Natl. Acad. Sci. U. S. A. 107 (2010) 13,713–13,717, http://dx.doi.org/10.1073/pnas.1005415107.
[53] S.A. Pabit, H. Roder, S.J. Hagen, Internal friction controls the speed of protein folding from a compact configuration†, Biochemistry. 43 (2004) 12,532–12,538, http://dx.doi.org/10.1021/bi048822m.
[54] L.E. Rosen, S.V. Kathuria, C.R. Matthews, O. Bilsel, S. Marqusee, Non-native structure appears in microseconds during the folding of *E. coli* RNase H, J. Mol. Biol. 427 (2015) 443–453, http://dx.doi.org/10.1016/j.jmb.2014.10.003.
[55] A.K. Patra, J.B. Udgaonkar, Characterization of the folding and unfolding reactions of single-chain monellin: evidence for multiple intermediates and competing pathways, Biochemistry. 46 (2007) 11,727–11,743.
[56] S.K. Jha, A. Dasgupta, P. Malhotra, J.B. Udgaonkar, Identification of multiple folding pathways of monellin using pulsed thiol labeling and mass spectrometry, Biochemistry. 50 (2011) 3062–3074, http://dx.doi.org/10.1021/bi1006332.
[57] S.K. Jha, D. Dhar, G. Krishnamoorthy, J.B. Udgaonkar, Continuous dissolution of structure during the unfolding of a small protein, Proc. Natl. Acad. Sci. 106 (2009) 11,113–11,118, http://dx.doi.org/10.1073/pnas.0812564106.
[58] S.J. Hagen, J. Hofrichter, A. Szabo, W.A. Eaton, Diffusion-limited contact formation in unfolded cytochrome *c*: estimating the maximum rate of protein folding, Proc. Natl. Acad. Sci. U. S. A. 93 (1996) 11,615–11,617.
[59] T.A. Laurence, X. Kong, M. Jäger, S. Weiss, Probing structural heterogeneities and fluctuations of nucleic acids and denatured proteins, Proc. Natl. Acad. Sci. U. S. A. 102 (2005) 17,348–17,353, http://dx.doi.org/10.1073/pnas.0508584102.
[60] H. Maity, G. Reddy, Folding of protein L with implications for collapse in the denatured state ensemble, J. Am. Chem. Soc. 138 (2016) 2609–2616, http://dx.doi.org/10.1021/jacs.5b11300.
[61] N.C. Fitzkee G.D. Rose, Reassessing Random-Coil Statistics in Unfolded Proteins, Proc. Natl. Acad. Sci. 101 (2004) 12497–12502.
[62] T. Uzawa, T. Kimura, K. Ishimori, I. Morishima, T. Matsui, M. Ikeda-Saito, et al., Time-resolved small-angle X-ray scattering investigation of the folding dynamics of heme oxygenase: implication of the scaling relationship for the submillisecond intermediates of protein folding, J. Mol. Biol. 357 (2006) 997–1008, http://dx.doi.org/10.1016/j.jmb.2005.12.089.
[63] H. Hofmann, A. Soranno, A. Borgia, K. Gast, D. Nettels, B. Schuler, Polymer scaling laws of unfolded and intrinsically disordered proteins quantified with single-molecule spectroscopy, Proc. Natl. Acad. Sci. 109 (2012) 16,155–16,160.
[64] W.Y. Yang, M. Gruebele, Folding at the speed limit, Nature. 423 (2003) 193–197, http://dx.doi.org/10.1038/nature01609.
[65] P. Li, F.Y. Oliva, A.N. Naganathan, V. Munoz, Dynamics of one-state downhill protein folding, Proc. Natl. Acad. Sci. U. S. A. 106 (2009) 103–108 (http://www.pnas.org/content/106/1/103.abstract).
[66] J. Kubelka, J. Hofrichter, W.a. Eaton, The protein folding "speed limit", Curr. Opin. Struct. Biol. 14 (2004) 76–88, http://dx.doi.org/10.1016/j.sbi.2004.01.013.
[67] A.N. Naganathan, U. Doshi, V. Muñoz, Protein folding kinetics: barrier effects in chemical and thermal denaturation experiments, J. Am. Chem. Soc. 129 (2007) 5673–5682, http://dx.doi.org/10.1021/ja0689740.
[68] G. Ziv, D. Thirumalai, G. Haran, Collapse transition in proteins, Phys. Chem. Chem. Phys. 11 (2009) 83–93, http://dx.doi.org/10.1039/b813961j.
[69] K.W. Plaxco, I.S. Millett, D.J. Segel, S. Doniach, D. Baker, Chain collapse can occur concomitantly with the rate-limiting step in protein folding, Nat. Struct. Mol. Biol. 6 (1999) 554–556, http://dx.doi.org/10.1038/9329.
[70] J. Jacob, B. Krantz, R.S. Dothager, P. Thiyagarajan, T.R. Sosnick, Early collapse is not an obligate step in protein folding, J. Mol. Biol. 338 (2004) 369–382, http://dx.doi.org/10.1016/j.jmb.2004.02.065.
[71] T.Y. Yoo, S.P. Meisburger, J. Hinshaw, L. Pollack, G. Haran, T.R. Sosnick, et al., Small-angle X-ray scattering and single-molecule FRET spectroscopy produce highly divergent views of the low-denaturant unfolded state, J. Mol. Biol. 418 (2012) 226–236, http://dx.doi.org/10.1016/j.jmb.2012.01.016.
[72] S.J. Hagen, W.a. Eaton, Two-state expansion and collapse of a polypeptide, J. Mol. Biol. 297 (2000) 781–789, http://dx.doi.org/10.1006/jmbi.2000.3508.
[73] S.V. Kathuria, C. Kayatekin, R. Barrea, E. Kondrashkina, R. Graceffa, L. Guo, et al., Microsecond barrier-limited chain collapse observed by time-resolved FRET and SAXS, J. Mol. Biol. 426 (2014) 1980–1994, http://dx.doi.org/10.1016/j.jmb.2014.02.020.
[74] B.R. Rami, G. Krishnamoorthy, J.B. Udgaonkar, Dynamics of the core tryptophan during the formation of a productive molten globule intermediate of barstar, Biochemistry. 42 (2003) 7986–8000, http://dx.doi.org/10.1021/bi030006b.
[75] C.J. Camacho, D. Thirumalai, Kinetics and thermodynamics of folding in model proteins, Proc. Natl. Acad. Sci. U. S. A. 90 (1993) 6369–6372 http://www.ncbi.nlm.nih.gov/pmc/articles/PMC46930/.
[76] A.S. Holehouse, K. Garai, N. Lyle, A. Vitalis, R.V. Pappu, Quantitative assessments of the distinct contributions of polypeptide backbone amides versus side chain groups to chain expansion via chemical denaturation, J. Am. Chem. Soc. 137 (2015) 2984–2995, http://dx.doi.org/10.1021/ja512062h.
[77] C.J. Camacho, D. Thirumalai, Minimum energy compact structures of random sequences of heteropolymers, Phys. Rev. Lett. 71 (1993) 2505.
[78] S.J. DeCamp, A.N. Naganathan, S.A. Waldauer, O. Bakajin, L.J. Lapidus, Direct observation of downhill folding of λ-repressor in a microfluidic mixer, Biophys. J. 97 (2009) 1772–1777, http://dx.doi.org/10.1016/j.bpj.2009.07.003.
[79] H. Roder, K. Maki, H. Cheng, Early events in protein folding explored by rapid mixing methods, Chem. Rev. 106 (2006) 1836–1861, http://dx.doi.org/10.1021/cr040430y.
[80] K.K. Sinha, J.B. Udgaonkar, Early events in protein folding, Curr. Sci. 96 (2009) 1053–1070.
[81] S.V. Kathuria, A. Chan, R. Graceffa, R. Paul Nobrega, C. Robert Matthews, T.C. Irving, et al., Advances in turbulent mixing techniques to study microsecond protein folding reactions, Biopolymers. 99 (2013) 888–896, http://dx.doi.org/10.1002/bip.22355.

[82] K. Teilum, K. Maki, B.B. Kragelund, F.M. Poulsen, H. Roder, Early kinetic intermediate in the folding of acyl-CoA binding protein detected by fluorescence labeling and ultrarapid mixing, Proc. Natl. Acad. Sci. 99 (2002) 9807–9812, http://dx.doi.org/10.1073/pnas.152321499.

[83] J.D. Bryngelson, P.G. Wolynes, Spin glasses and the statistical mechanics of protein folding, Proc. Natl. Acad. Sci. 84 (1987) 7524–7528 (http://www.pnas.org/content/84/21/7524.abstract).

[84] J.D. Bryngelson, J.N. Onuchic, N.D. Socci, P.G. Wolynes, Funnels, pathways, and the energy landscape of protein folding: a synthesis, Proteins Struct. Funct. Bioinf. 21 (1995) 167–195.

[85] K. Dill, H. Chan, From Levinthal to pathways to funnels, Nat. Struct. Mol. Biol. 4 (1997) 10–19, http://dx.doi.org/10.1038/nsb0197-10.

[86] K. Sridevi, G.S. Lakshmikanth, G. Krishnamoorthy, J.B. Udgaonkar, Increasing stability reduces conformational heterogeneity in a protein folding intermediate ensemble, J. Mol. Biol. 337 (2004) 699–711, http://dx.doi.org/10.1016/j.jmb.2003.12.083.

[87] S. Akiyama, S. Takahashi, K. Ishimori, I. Morishima, Stepwise formation of alpha-helices during cytochrome *c* folding, Nat. Struct. Biol. 7 (2000) 514–520, http://dx.doi.org/10.1038/75932.

[88] S.-H. Park, M.C.R. Shastry, H. Roder, Folding dynamics of the B1 domain of protein G explored by ultrarapid mixing, Nat. Struct. Mol. Biol. 6 (1999) 943–947, http://dx.doi.org/10.1038/13311.

[89] A.P. Capaldi, M.C.R. Shastry, C. Kleanthous, H. Roder, S.E. Radford, Ultrarapid mixing experiments reveal that Im7 folds via an on-pathway intermediate, Nat. Struct. Mol. Biol. 8 (2001) 68–72, http://dx.doi.org/10.1038/83074.

[90] L. Qiu, C. Zachariah, S.J. Hagen, Fast chain contraction during protein folding: "foldability" and collapse dynamics, Phys. Rev. Lett. 90 (2003) 168,103, http://dx.doi.org/10.1103/PhysRevLett.90.168103.

[91] T.R. Sosnick, M.D. Shtilerman, L. Mayne, S.W. Englander, Ultrafast signals in protein folding and the polypeptide contracted state, Proc. Natl. Acad. Sci. 94 (1997) 8545–8550 (http://www.pnas.org/content/94/16/8545.abstract).

[92] P.X. Qi, T.R. Sosnick, S.W. Englander, The burst phase in ribonuclease A folding and solvent dependence of the unfolded state, Nat. Struct. Mol. Biol. 5 (1998) 882–884, http://dx.doi.org/10.1038/2321.

[93] K. Nakagawa, Y. Yamada, Y. Matsumura, S. Tsukamoto, M. Yamamoto-Ohtomo, H. Ohtomo, et al., Relationship between chain collapse and secondary structure formation in a partially folded protein, Biopolymers. 101 (2014) 651–658, http://dx.doi.org/10.1002/bip.22433.

[94] S.K. Jha, J.B. Udgaonkar, Direct evidence for a dry molten globule intermediate during the unfolding of a small protein, Proc. Natl. Acad. Sci. 106 (2009) 12,289–12,294, http://dx.doi.org/10.1073/pnas.0905744106.

[95] G.S. Lakshmikanth, K. Sridevi, G. Krishnamoorthy, J.B. Udgaonkar, Structure is lost incrementally during the unfolding of barstar, Nat. Struct. Mol. Biol. 8 (2001) 799–804, http://dx.doi.org/10.1038/nsb0901-799.

[96] L.A. Campos, M. Sadqi, J. Liu, X. Wang, D.S. English, V. Muñoz, Gradual disordering of the native state on a slow two-state folding protein monitored by single-molecule fluorescence spectroscopy and NMR, J. Phys. Chem. B. 117 (2013) 13,120–13,131, http://dx.doi.org/10.1021/jp403051k.

[97] S. Mukhopadhyay, P.K. Nayak, J.B. Udgaonkar, G. Krishnamoorthy, Characterization of the formation of amyloid protofibrils from barstar by mapping residue-specific fluorescence dynamics, J. Mol. Biol. 358 (2006) 935–942, http://dx.doi.org/10.1016/j.jmb.2006.02.006.

[98] V.R. Agashe, J.B. Udgaonkar, Thermodynamics of denaturation of barstar: evidence for cold denaturation and evaluation of the interaction with guanidine hydrochloride, Biochemistry. 34 (1995) 3286–3299 (http://www.ncbi.nlm.nih.gov/pubmed/7880824).